

Implications evinced by the phase diagram, anisotropy, magnetic penetration depths, isotope effects and conductivities of cuprate superconductors

T. Schneider and H. Keller

*Physik-Institut der Universität Zürich, Winterthurerstrasse 190,
CH-8057 Zürich, Switzerland*

Anisotropy, thermal and quantum fluctuations and their dependence on dopant concentration appear to be present in all cuprate superconductors, interwoven with the microscopic mechanisms responsible for superconductivity. Here we review anisotropy, in-plane and c-axis penetration depths, isotope effect and conductivity measurements to reassess the universal behavior of cuprates as revealed by the doping dependence of these phenomena and of the transition temperature.

Establishing and understanding the phase diagram of cuprate superconductors in the temperature-dopant concentration plane is one of the major challenges in condensed matter physics. Superconductivity is derived from the insulating and antiferromagnetic parent compounds by partial substitution of ions or by adding or removing oxygen. For instance La_2CuO_4 can be doped either by alkaline earth ions or oxygen to exhibit superconductivity. The empirical phase diagram of $\text{La}_{2-x}\text{Sr}_x\text{CuO}_4$ [1–9] depicted in Fig. 1a shows that after passing the so called underdoped limit ($x_u \approx 0.047$), T_c reaches its maximum value $T_c(x_m)$ at $x_m \approx 0.16$. With further increase of x , T_c decreases and finally vanishes in the overdoped limit $x_o \approx 0.273$. This phase transition line is thought to be a generic property of cuprate superconductors [10] and is well described by the empirical relation

$$T_c(x) = T_c(x_m) \left(1 - 2 \left(\frac{x}{x_m} - 1 \right)^2 \right) = \frac{2T_c(x_m)}{x_m^2} (x - x_u)(x_o - x), \quad (1)$$

proposed by Presland *et al.* [11]. Approaching the endpoints along the x -axis, $\text{La}_{2-x}\text{Sr}_x\text{CuO}_4$ undergoes at zero temperature doping tuned quantum phase transitions. As their nature is concerned, resistivity measurements reveal a quantum superconductor to insulator (QSI) transition in the underdoped limit [12–18] and in the overdoped limit a quantum superconductor to normal state (QSN) transition [12].

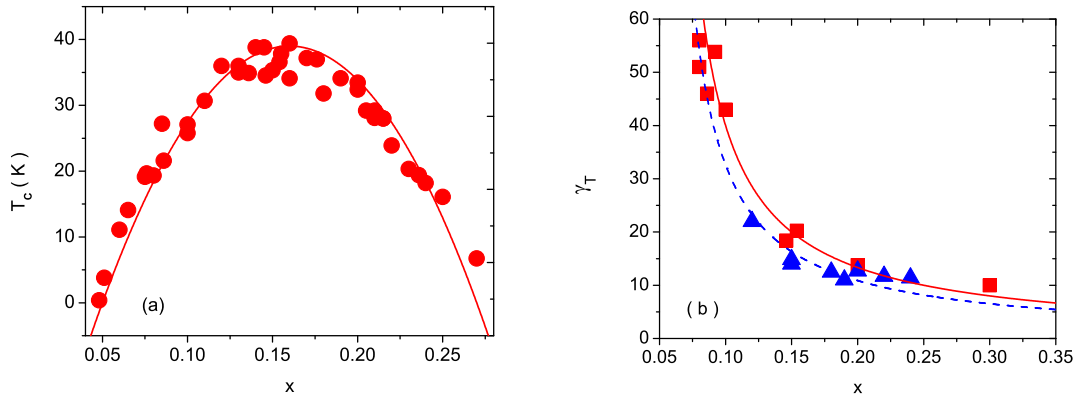


FIG. 1. (a) Variation of T_c for $\text{La}_{2-x}\text{Sr}_x\text{CuO}_4$. Experimental data taken from [1–9]. The solid line is Eq.(1) with $T_c(x_m) = 39$ K. (b) γ_T versus x for $\text{La}_{2-x}\text{Sr}_x\text{CuO}_4$. The squares are the experimental data for γ_{T_c} [1,2,4,6,7] and the triangles for $\gamma_{T=0}$ [8,9]. The solid curve and dashed lines are Eq.(2) with $\gamma_{T_c,0} = 2$ and $\gamma_{T=0,0} = 1.63$.

Another essential experimental fact is the doping dependence of the anisotropy. In tetragonal cuprates it is defined as the ratio $\gamma = \xi_{ab}/\xi_c$ of the correlation lengths parallel (ξ_{ab}) and perpendicular (ξ_c) to CuO_2 layers (ab -planes). In the superconducting state it can also be expressed as the ratio $\gamma = \lambda_c/\lambda_{ab}$ of the London penetration depths due to supercurrents flowing perpendicular (λ_c) and parallel (λ_{ab}) to the ab -planes. Approaching a non-superconductor to superconductor transition ξ diverges, while in a superconductor to non-superconductor transition λ tends to infinity. In both cases, however, γ remains finite as long as the system exhibits anisotropic but genuine 3D behavior. There are two limiting cases: $\gamma = 1$ characterizes isotropic 3D- and $\gamma = \infty$ 2D-critical behavior. An instructive model where γ can be varied continuously is the anisotropic 2D Ising model [19]. When the coupling in the y direction

goes to zero, $\gamma = \xi_x/\xi_y$ becomes infinite, the model reduces to the 1D case, and T_c vanishes. In the Ginzburg-Landau description of layered superconductors the anisotropy is related to the interlayer coupling. The weaker this coupling is, the larger γ is. The limit $\gamma = \infty$ is attained when the bulk superconductor corresponds to a stack of independent slabs of thickness d_s . With respect to experimental work, a considerable amount of data is available on the chemical composition dependence of γ . At T_c it can be inferred from resistivity ($\gamma = \xi_{ab}/\xi_c = \sqrt{\rho_{ab}/\rho_c}$) and magnetic torque measurements, while in the superconducting state it follows from magnetic torque and penetration depth ($\gamma = \lambda_c/\lambda_{ab}$) data. In Fig. 1b we displayed the doping dependence of γ_T evaluated at T_c (γ_{T_c}) and $T = 0$ ($\gamma_{T=0}$). As the dopant concentration is reduced, γ_{T_c} and $\gamma_{T=0}$ increase systematically, and tend to diverge in the underdoped limit. Thus the temperature range where superconductivity occurs shrinks in the underdoped regime with increasing anisotropy. This competition between anisotropy and superconductivity raises serious doubts whether 2D mechanisms and models, corresponding to the limit $\gamma_T = \infty$, can explain the essential observations of superconductivity in the cuprates. From Fig. 1 it is also seen that $\gamma_T(x)$ is well described by

$$\gamma_T(x) = \frac{\gamma_{T,0}}{x - x_u}, \quad (2)$$

where $\gamma_{T,0}$ is the quantum critical amplitude. Having also other cuprate families in mind, it is convenient to express the dopant concentration in terms of T_c . From Eqs.(1) and(2) we obtain the correlation between T_c and γ_T :

$$\frac{T_c(x)}{T_c(x_m)} = 1 - \left(\frac{\gamma_T(x_m)}{\gamma_T(x)} - 1 \right)^2, \quad \gamma_T(x_m) = \frac{\gamma_{T,0}}{x_m - x_u} \quad (3)$$

Provided that this empirical correlation is not merely an artefact of $\text{La}_{2-x}\text{Sr}_x\text{CuO}_4$, it gives a universal perspective on the interplay of anisotropy and superconductivity, among the families of cuprates, characterized by $T_c(x_m)$ and $\gamma_T(x_m)$. For this reason it is essential to explore its generic validity. In practice, however, there are only a few additional compounds, including $\text{HgBa}_2\text{CuO}_{4+\delta}$ [20], for which the dopant concentration can be varied continuously throughout the entire doping range. It is well established, however, that the substitution of magnetic and nonmagnetic impurities, depress T_c of cuprate superconductors very effectively [21,22]. To compare the doping and substitution driven variations of the anisotropy, we depicted in Fig. 2 the plot $T_c(x)/T_c(x_m)$ versus $\gamma_T(x_m)/\gamma_T(x)$ for a variety of cuprate families. The collapse of the data on the parabola, which is the empirical relation (3), reveals that this scaling form appears to be universal. Thus, given a family of cuprate superconductors, characterized by $T_c(x_m)$ and $\gamma_T(x_m)$, it gives a universal perspective on the interplay between anisotropy and superconductivity.

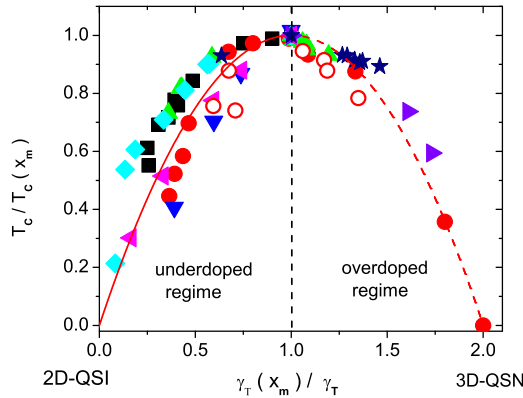


FIG. 2. $T_c(x)/T_c(x_m)$ versus $\gamma_T(x_m)/\gamma_T(x)$ for various cuprate families: $\text{La}_{2-x}\text{Sr}_x\text{CuO}_4$ (\bullet , $T_c(x_m) = 37\text{K}$, $\gamma_{T_c}(x_m) = 20$) [1,2,4,6,7], (\circ , $T_c(x_m) = 37\text{K}$, $\gamma_{T=0}(x_m) = 14.9$) [8,9], $\text{HgBa}_2\text{CuO}_{4+\delta}$ (\blacktriangle , $T_c(x_m) = 95.6\text{K}$, $\gamma_{T_c}(x_m) = 27$) [20], $\text{Bi}_2\text{Sr}_2\text{CaCu}_2\text{O}_{8+\delta}$ (\star , $T_c(x_m) = 84.2\text{K}$, $\gamma_{T_c}(x_m) = 133$) [23], $\text{YBa}_2\text{Cu}_3\text{O}_{7-\delta}$ (\blacklozenge , $T_c(x_m) = 92.9\text{K}$, $\gamma_{T_c}(x_m) = 8$) [24], $\text{YBa}_2(\text{Cu}_{1-y}\text{Fe}_y)_3\text{O}_{7-\delta}$ (\blacksquare , $T_c(x_m) = 92.5\text{K}$, $\gamma_{T_c}(x_m) = 9$) [25], $\text{Y}_{1-y}\text{Pr}_y\text{Ba}_2\text{Cu}_3\text{O}_{7-\delta}$ (\blacktriangledown , $T_c(x_m) = 91\text{K}$, $\gamma_{T_c}(x_m) = 9.3$) [26], $\text{BiSr}_2\text{Ca}_{1-y}\text{Pr}_y\text{Cu}_2\text{O}_8$ (\blacktriangleleft , $T_c(x_m) = 85.4\text{K}$, $\gamma_{T=0}(x_m) = 94.3$) [27] and $\text{YBa}_2(\text{Cu}_{1-y}\text{Zn}_y)_3\text{O}_{7-\delta}$ (\blacktriangleright , $T_c(x_m) = 92.5\text{K}$, $\gamma_{T=0}(x_m) = 9$) [28]. The solid and dashed curves are Eq.(3), marking the flow from the maximum T_c to QSI and QSN criticality, respectively.

Close to 2D-QSI criticality various properties are not independent but related by [13–18]

$$T_c = \frac{\Phi_0^2 R_2}{16\pi^3 k_B \lambda_{ab}^2(0)} \frac{d_s}{\lambda_{ab}^2(0)} \propto \gamma_T^{-z} \propto \delta^{z\bar{\nu}}, \quad (4)$$

independently of the nature of the putative quantum critical point. k_B is the Boltzmann constant, Φ_0 the elementary flux quantum, $\lambda_{ab}(0)$ the zero temperature in-plane penetration depth, z is the dynamic critical exponent, d_s the thickness of the sheets, and $\overline{\nu}$ the correlation length critical exponent of the 2D-QSI transitions. δ measures the distance from the critical point along the x axis (see Fig.1a), and R_2 is a universal number. Since $T_c \propto d_s/\lambda_{ab}^2(0) \propto n_s^\square$, where n_s^\square is the aerial superfluid density, is a characteristic 2D property, it also applies to the onset of superfluidity in ^4He films adsorbed on disordered substrates, where it is well confirmed [29]. A great deal of experimental work has also been done in cuprates on the so called Uemura plot, revealing an empirical correlation between T_c and $d_s/\lambda_{ab}^2(0)$ [30]. Approaching 2D-QSI criticality, the data of a given family tends to fall on a straight line, consistent with Eq.(4). Differences in the slope reflect the family dependent value of d_s , the thickness of the sheets, becoming independent in the 2D limit [14–18]. The relevance of d_s was also confirmed in terms of the relationship between the isotope effect on T_c and $1/\lambda_{ab}^2$ [16,31]. Moreover, together with the scaling form (4) the empirical relation (1) implies 2D-QSI and 3D-QSN transitions with $z\overline{\nu} = 1$, while the empirical behavior of the anisotropy (Eqs.(2) and (3)) require $\overline{\nu} = 1$ at the 2D-QSI criticality. Thus, the empirical correlations point to a 2D-QSI transition with $z = 1$ and $\overline{\nu} = 1$. These estimates coincide with the theoretical prediction for a 2D disordered bosonic system with long-range Coulomb interactions, where $z = 1$ and $\overline{\nu} \simeq 1$ [32–34]. Here the loss of superfluidity is due to the localization of the pairs, which ultimately drives the transition. From the scaling relation (4) it is seen that measurements of the out of plane penetration depth of sufficiently underdoped systems allow to estimate the dynamic critical exponent z directly, in terms of $T_c \propto (1/\lambda_c^2(0))^{z/(z+2)}$, which follows from Eq.(4) with $\gamma_T = \lambda_c(0)/\lambda_{ab}(0)$. In Fig.3 we displayed the data of Hosseini *et al.* [35] for heavily underdoped $\text{YBa}_2\text{Cu}_3\text{O}_{7-\delta}$ single crystals. The solid line is $1/\lambda_c^2(T=0) = 2.44 \cdot 10^{-4} T_c^3$ and uncovers the consistency with the 2D-QSI scaling relation $T_c \propto (1/\lambda_c^2(0))^{z/(z+2)}$ with $z = 1$.

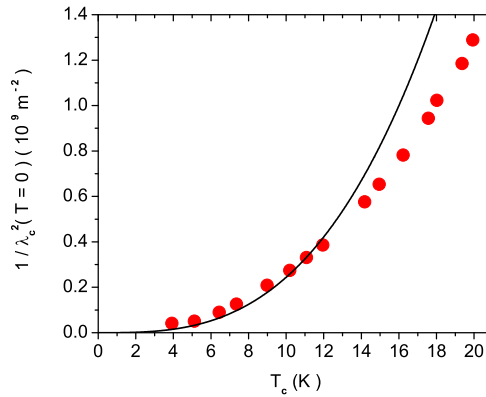


FIG. 3. $1/\lambda_c^2(T=0)$ vs. T_c for $\text{YBa}_2\text{Cu}_3\text{O}_{6+x}$ single crystals, taken from Hosseini *et al.* [35]. The solid line is $1/\lambda_c^2(T=0) = 2.44 \cdot 10^{-4} T_c^3$ and indicates the consistency with the 2D-QSI scaling relation $T_c \propto (1/\lambda_c^2(0))^{z/(z+2)}$ and $z = 1$.

Furthermore, Hosseini *et al.* [35] found that at low temperature $1/\lambda_c^2(T) - 1/\lambda_c^2(0)$ is nearly doping independent. Given this behavior close to the 2D-QSI transition, scaling predicts that in leading order $1/\lambda_c^2(T) - 1/\lambda_c^2(0) \propto T^3$ holds, in good agreement with the experimental data displayed in Fig. 4. As the in-plane penetration depth is concerned, there is mounting experimental evidence that $1/\lambda_{ab}^2(T) - 1/\lambda_{ab}^2(0)$ is in the limit $T \rightarrow 0$ nearly doping independent as well [15]. In this case 2D-QSI scaling predicts in leading order $1/\lambda_{ab}^2(T) - 1/\lambda_{ab}^2(0) \propto T$, in agreement with the experimental data of numerous cuprates [15].

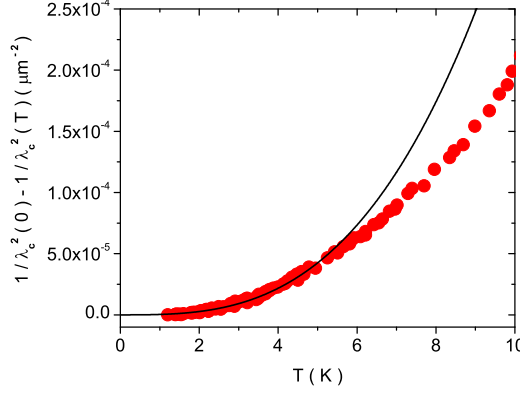


FIG. 4. $1/\lambda_c^2(T) - 1/\lambda_c^2(0)$ vs. T for $\text{YBa}_2\text{Cu}_3\text{O}_{6+x}$ single crystals, with T_c values $\approx 20.2, 19.5, 18.2, 17.8, 16.4$, and 15.1K taken from Hosseini *et al.* [35]. The solid curve is $1/\lambda_c^2(T) - 1/\lambda_c^2(0) = 3.4 \cdot 10^{-7} T^3$.

We have seen that the doping tuned flow to the 2D-QSI critical point is associated with a depression of T_c and an enhancement of γ_T . It implies that when the 2D-QSI transition is approached, a non vanishing T_c is inevitably associated with an anisotropic but 3D condensation mechanism, because γ_T is finite for $T_c > 0$ (see Figs. 1 and 2). This represents a serious problem for 2D models [36] as candidates to explain superconductivity in the cuprates, and serves as a constraint on future work toward a complete understanding. Note that the vast majority of theoretical models focus on a single Cu-O plane, i.e., on the limit of zero intracell and intercell c-axis coupling.

Since Eq.(4) is universal, it also implies that the changes ΔT_c , Δd_s and $\Delta(1/\lambda_{ab}^2(T=0))$, induced by pressure or isotope exchange are not independent, but related by

$$\frac{\Delta T_c}{T_c} = \frac{\Delta d_s}{d_s} + \frac{\Delta(1/\lambda_{ab}^2(0))}{(1/\lambda_{ab}^2(0))} = \frac{\Delta d_s}{d_s} - 2 \frac{\Delta(\lambda_{ab}(0))}{\lambda_{ab}(0)}. \quad (5)$$

In particular, for the oxygen isotope effect (^{16}O vs. ^{18}O) of a physical quantity X the relative isotope shift is defined as $\Delta X/X = (^{18}X - ^{16}X)/^{18}X$. In Fig. 5 we show the data for the oxygen isotope effect in $\text{La}_{2-x}\text{Sr}_x\text{CuO}_4$ [37,38], $\text{Y}_{1-x}\text{Pr}_x\text{Ba}_2\text{Cu}_3\text{O}_{7-\delta}$ [38–40] and $\text{YBa}_2\text{Cu}_3\text{O}_{7-\delta}$ [38,41], extending from the underdoped to the optimally doped regime, in terms of $\Delta(\lambda_{ab}(0))/\lambda_{ab}(0)$ vs. $-\Delta T_c/T_c$.

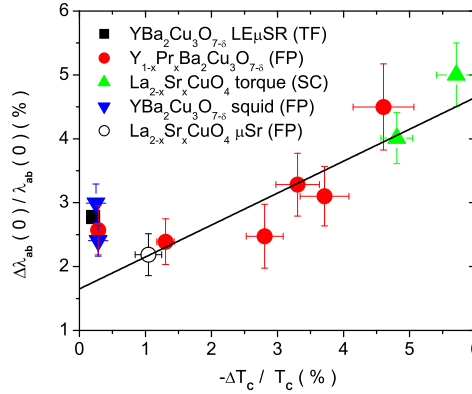


FIG. 5. Data for the oxygen isotope effect in underdoped $\text{La}_{2-x}\text{Sr}_x\text{CuO}_4$ (\circ : $x=0.15$ [38], \blacktriangle : $x=0.08, 0.086$ [37], $\text{Y}_{1-x}\text{Pr}_x\text{Ba}_2\text{Cu}_3\text{O}_{7-\delta}$ (\bullet : $x=0, 0.2, 0.3, 0.4$) [38–40] and $\text{YBa}_2\text{Cu}_3\text{O}_{7-\delta}$ (\blacktriangledown [38], \blacksquare [41]) in terms of $\Delta(\lambda_{ab}(0))/\lambda_{ab}(0)$ vs. $-\Delta T_c/T_c$. The solid line indicates the flow to 2D-QSI criticality and provides with Eq.(5) an estimate for the oxygen isotope effect on d_s , namely $\Delta d_s/d_s = 3.3(4)\%$.

It is evident that there is a correlation between the isotope effect on T_c and $\lambda_{ab}(0)$ which appears to be universal for all cuprate families. Indeed, the solid line indicates the flow to the 2D-QSI transition and provides with Eq.(5) an estimate for the oxygen isotope effect on d_s , namely $\Delta d_s/d_s = 3.3(4)\%$. Approaching optimum doping, this

contribution renders the isotope effect on T_c considerably smaller than that on $\lambda_{ab}(0)$. Indeed, even in nearly optimally doped $\text{YBa}_2\text{Cu}_3\text{O}_{7-\delta}$, where $\Delta T_c/T_c = -0.26(5)\%$, a substantial isotope effect on the in-plane penetration depth, $\Delta\lambda_{ab}(0)/\lambda_{ab}(0) = -2.8(1.0)\%$, has been established by direct observation, using the novel low-energy muon-spin rotation technique [41]. Note that these findings have been obtained using various experimental techniques on powders, thin films and single crystals.

In this context it is important to recognize that the substantial isotope effect on the in-plane penetration depth is incompatible with the Migdal-Eliashberg (ME) [42] of the electron-phonon interaction [43]. Since the lattice parameters remain essentially unaffected [44,45] by isotope exchange, while the dynamics associated with the mass of the respective ions is modified, the substantial isotope effect on the zero temperature penetration depth requires a renormalization of the normal state Fermi velocity $\mathbf{v}_F \rightarrow \tilde{\mathbf{v}}_F = \mathbf{v}_F/(1+f)$ where \mathbf{v}_F is the bare velocity and f the electron-phonon coupling constant. However, in the Migdal-Eliashberg [42] treatment of the electron-phonon interaction f is independent of the ionic masses and assumed to be small [46,47]. This is true if the parameter $\omega_0 f/E_F$ is small, where ω_0 is the relevant phonon frequency and E_F the Fermi energy. Thus the isotope effect on the penetration depth is expected to be small, of the order of the adiabatic parameter $\tilde{\gamma} = \omega_0/E_F \ll 1$. The ME theory retains terms only of order 0. Cuprates, however, have Fermi energies much smaller than those of conventional metals [48] so that $\tilde{\gamma}$ is no longer negligible small. In any case the substantial isotope effect on the in-plane penetration depth uncovers the coupling between local lattice distortions and superfluidity and the failure of the Migdal-Eliashberg (ME) treatment of the electron-phonon interaction, predicting $1/\lambda^2(0)$ to be independent of the ionic masses [42]. Evidence for this coupling emerges from the oxygen isotope effect on d_s , the thickness of the superconducting sheets, while the lattice parameters remain unaffected. Indeed, the relative shift, $\Delta d_s/d_s \approx 3.3(4)\%$, apparent in Fig.5, implies local oxygen distortions which do not modify the lattice parameters but are coupled to the superfluid. Although the majority opinion on the mechanism of superconductivity in the cuprates is that it occurs via a purely electronic mechanism involving spin excitations, and lattice degrees of freedom are supposed to be irrelevant, the relative isotope shift $\Delta d_s/d_s \approx 3.3(4)\%$ uncovers clearly the existence and relevance of the coupling between the superfluid and local lattice distortions.

Finally we turn to the finite temperature critical behavior. Close to the critical temperature T_c of the superconductor to normal state transition, in a regime roughly given by the Ginzburg criterion [14,49–51], order parameter fluctuations dominate critical properties. In recent years, the effect of the charge of the superconducting order parameter in this regime in three dimensions has been studied extensively [52–59,61]. While for strong type-I materials, the coupling of the order parameter to transverse gauge field fluctuations is expected to render the transition first order [53], it is well-established that strong type-II materials should exhibit a continuous phase transition, and that sufficiently close to T_c , the charge of the order parameter is relevant [55–61]. However, in cuprate superconductors within the fluctuation dominated regime, the region close to T_c , where the system crosses over to the regime of charged fluctuations turns out to be too narrow to access. For instance, optimally doped $\text{YBa}_2\text{Cu}_3\text{O}_{7-\delta}$, while possessing an extended regime of critical fluctuations, is too strongly type-II to observe charged critical fluctuations [14,49–51,62]. Indeed, the effective dimensionless charge $\tilde{e} = \xi/\lambda = 1/\kappa$ is small in strongly type II superconductors ($\kappa \gg 1$). The crossover upon approaching T_c is thus initially to the critical regime of a weakly charged superfluid where the fluctuations of the order parameter are essentially those of an uncharged superfluid or XY-model [49]. Furthermore, there is the inhomogeneity induced finite size effect which renders the asymptotic critical regime unattainable [63–65]. However, underdoped cuprates could open a window onto this new regime because κ_{ab} is expected to become rather small. As outlined above, in this regime cuprates undergo a quantum superconductor to insulator transition [14–18] and correspond to a 2D disordered bosonic system with long-range coulomb interactions. Close to this quantum transition T_c , λ_{ab} and ξ_{ab} scale as $T_c \propto \lambda_{ab}^{-2} \propto \xi_{ab}^{-z} \propto \lambda_c^{-2(z+2)/z}$ [14–18], while $\xi_c \rightarrow d_s$. These relations yield with the dynamic critical exponent $z = 1$ [14,18,32–34], $\kappa_{ab} \propto T_c^{1/2}$ and $\kappa_c \propto T_c^{-3/2}$. Noting that T_c decreases by approaching the underdoped limit, the in-plane penetration depth appears to be a potential candidate to observe charged criticality in sufficiently homogeneous and underdoped cuprates, while the c-axis counterpart is expected to exhibit neutral critical behavior.

When charged fluctuations dominate the in-plane penetration depth and the correlation length are related by [57–61]

$$\lambda_{ab} = \kappa_{ab}\xi_{ab}, \quad \lambda_{ab} = \lambda_{0ab}|t|^{-\nu}, \quad \nu \simeq 2/3, \quad (6)$$

contrary to the uncharged case, where $\lambda \propto \sqrt{\xi}$ and with that

$$\lambda_{ab} = \lambda_{0ab}|t|^{-\nu/2}, \quad (7)$$

where $t = T/T_c - 1$. In a plot $(d \ln \lambda_{ab}/dT)^{-1}$ vs. T charged critical behavior is then uncovered in terms of a temperature range where the data falls on a line with slope $1/\nu \simeq 3/2$, while in the neutral (3D-XY) case it collapses

on a line with slope $2/\nu \simeq 3$. Clearly, in an inhomogeneous system the phase transition is rounded and $(d \ln \lambda_{ab}/dT)^{-1}$ does not vanish at T_c . In Fig. 6 we displayed $(T_c d \ln \lambda_{ab}/dT)^{-1}$ vs. t for $\text{YBa}_2\text{Cu}_3\text{O}_{6.59}$ with applied hydrostatic pressures of 0.5kbar and 10.5kbar, derived from the measured in-plane penetration depth data of ref. [66]. The solid line with slope $1/\nu \simeq 3/2$ indicates according to Eq. (6) the charged criticality in homogeneous systems with $T_c = 57.82\text{K}$ and $T_c = 61.1\text{K}$. Although the charged criticality is attained there is no sharp transition because λ_{ab} does not diverge at T_c . Inhomogeneities prevent the correlation length $\xi_{ab} = \lambda_{ab}/\kappa_{ab}$ to grow beyond the spatial extent L_{ab} of the homogenous domains in the ab -plane. For a discussion of the associated finite size effect we refer to ref. [66]. In any case these measurements clearly reveal that the temperature dependence of the in-plane penetration depth opens a window onto charged criticality at finite temperature in underdoped cuprates.

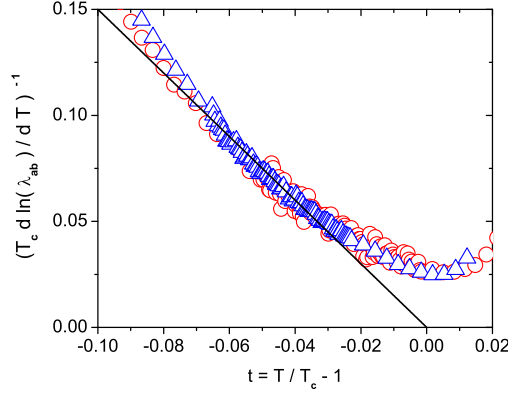


FIG. 6. $(T_c d \ln \lambda_{ab}/dT)^{-1}$ with λ_{ab} in μm vs. t for $\text{YBa}_2\text{Cu}_3\text{O}_{6.59}$ under hydrostatic pressure of 0.5kbar (\triangle) and 10.5kbar (\circ) taken from ref. [66]. The straight line with slope $1/\nu \simeq 3/2$ corresponds according to Eq. (6) to charged critical behavior with $T_c = 57.82\text{K}$ and $T_c = 61.1\text{K}$.

Extended c-axis penetration depth measurements on $\text{YBa}_2\text{Cu}_3\text{O}_{6+x}$ single crystals with T_c 's ranging from 4 to 20K have been performed by Hosseini *et al.* [35]. In Fig. 7 we displayed their data for the sample with $T_c \approx 19.75\text{K}$ in terms λ_c^{-2} and $(d \ln \lambda_c^{-2}/dT)^{-1}$ vs. T . The solid curve is $\lambda_c^{-2} = \lambda_{0c}^{-2} (1 - T/T_c)^\nu$ with $T_c = 19.75\text{K}$ and $\lambda_{0c}^{-2} = 2.15$ (10^9m^{-2}) and the dashed one $(d \ln \lambda_c^{-2}/dT)^{-1} = -1/\nu (T_c - T)$ with $\nu \simeq 2/3$.

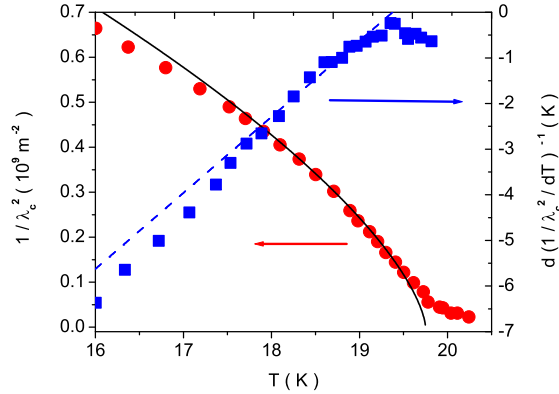


FIG. 7. λ_c^{-2} and $(d \ln \lambda_c^{-2}/dT)^{-1}$ vs. T for a $\text{YBa}_2\text{Cu}_3\text{O}_{6+x}$ single crystal derived from the data of Hosseini *et al.* [35]. The solid curve is $\lambda_c^{-2} = \lambda_{0c}^{-2} (1 - T/T_c)^\nu$ with $T_c = 19.75\text{K}$ and $\lambda_{0c}^{-2} = 2.15$ (10^9m^{-2}) and the dashed one $(d \ln \lambda_c^{-2}/dT)^{-1} = -1/\nu (T_c - T)$ with $\nu \simeq 2/3$. They indicate according to Eq. (7) the leading uncharged (3D-XY) critical behavior.

They indicate according to Eq. (7) the leading uncharged (3D-XY) critical behavior. Noting that in this underdoped regime the anisotropy $\gamma = \lambda_c/\lambda_{ab}$ is rather large (see Fig. 2) the critical regime where thermal 3D fluctuations dominate will be compared to optimum doping much narrower. Here it extends to $t \approx 77/93.7 - 1 \simeq -0.18$ [62].

Nevertheless, a glance to Fig. 7 shows that the 3D-XY critical regime is attained for $18\text{K} \lesssim T \lesssim 19\text{K}$, corresponding to $0.09 \gtrsim |t| \gtrsim 0.04$. The tail above 19K is attributable to an inhomogeneity induced finite size effect. Indeed, according to the scaling relation $\kappa_c \propto T_c^{-3/2}$ it is unlikely that the crossover to charged criticality is attainable. In contrast and consistent with $\kappa_{ab} \propto T_c^{1/2}$ charged criticality turned out to be accessible in the ab -plane penetration depth.

We have seen that the linear relationship between T_c and $1/\lambda_{ab}^2(0)$ in the underdoped regime, referred to as the Uemura relation, is a consequence of the dimensional crossover associated with the flow to the 2D-QSI transition (see Eq.(4). To illustrate this behavior we displayed in Fig. 8 T_c vs. $1/\lambda_{ab}^2(0)$ for $\text{La}_{2-x}\text{Sr}_x\text{CuO}_4$. The straight line is Eq.(4) in terms of $T_c = 25\lambda_{ab}^{-2}(0)$ and the arrow indicates the flow to the 2D-QSI criticality. However, approaching the optimally doped regime, where T_c reaches its maximum value (see Fig. 1), the observed T_c 's are systematically lower than the 2D-QSI line and this trend continues in the overdoped regime.

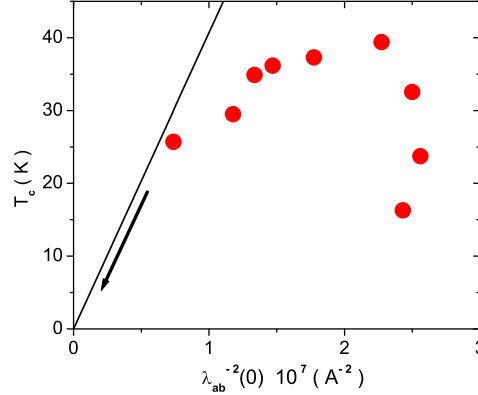


FIG. 8. T_c vs. $1/\lambda_{ab}^2(0)$ for $\text{La}_{2-x}\text{Sr}_x\text{CuO}_4$. Data taken from Uemura *et al.* [30,67] and Panagopoulos *et al.* [9]. The straight line is Eq.(4) with $R_2 d_s = 6.5\text{\AA}$ and the arrow indicates the flow to 2D-QSI transition criticality.

To provide an understanding we invoke 3D-XY universality expected to hold along the phase transition line, $T_c(x)$ in $\text{La}_{2-x}\text{Sr}_x\text{CuO}_4$ (see Fig. 1), as long as the charge of the pairs can be neglected. In this case the transition temperature T_c and the critical amplitudes of the penetration depths λ_{ab0} and transverse correlation lengths ξ_{ab0}^{tr} are related by [14,18]

$$k_B T_c = \frac{\Phi_0^2}{16\pi^3} \frac{\xi_{ab0}^{tr}}{\lambda_{ab0}^2} = \frac{\Phi_0^2}{16\pi^3} \frac{\xi_{c0}^{tr}}{\lambda_{c0}^2}, \quad (8)$$

where $\lambda_i^2(T) = \lambda_{i0}^2 (1 - T/T_c)^{-\nu}$ and $\xi_i^t(T) = \xi_{i0}^t (1 - T/T_c)^{-\nu}$ with $\nu \simeq 2/3$. For our purpose it is convenient to express the transverse correlation length to the correlation lengths above T_c in terms of [14,18,68]

$$\frac{\xi_{ab0}^{tr}}{\xi_{c0}} = f \approx 0.453, \quad \frac{\xi_{c0}^{tr}}{\xi_{ab0}} = \gamma f, \quad (9)$$

where the anisotropy is given by

$$\gamma^2 = \left(\frac{\lambda_{c0}}{\lambda_{ab0}} \right)^2 = \frac{\xi_{c0}^{tr}}{\xi_{ab0}^{tr}} = \left(\frac{\xi_{ab0}}{\xi_{c0}} \right)^2. \quad (10)$$

Combining Eqs.(8) and (9) we obtain the universal relation

$$T_c \lambda_{ab0}^2 = \frac{\Phi_0^2 f}{16\pi^3 k_B} \xi_{c0}. \quad (11)$$

It holds, as long as cuprates fall into the 3D-XY universality class, irrespective of the doping dependence of T_c , λ_{ab0}^2 and ξ_{c0} . For this reason it provides a sound basis for universal plots. However, there is the serious drawback that reliable experimental estimates for T_c and the critical amplitudes λ_{ab0} and ξ_{c0} measured on the same sample are not yet available. Nevertheless, some progress can be made by noting that in the underdoped regime, approaching the 2D-QSI transition the universal scaling forms (4) and (11) should match. This requires

$$f\xi_{c0} \rightarrow Rd_s, \quad (12)$$

so that away from 2D-QSI criticality

$$T_c \lambda_{ab}^2(0) \simeq \frac{\Phi_0^2 f}{16\pi^3 k_B} \xi_{c0}, \quad (13)$$

holds. Thus, when both T_c and $1/\lambda_{ab}^2(0)$ increase, T_c values below $T_c = (\Phi_0^2 R_2 / 6\pi^3 k_B) d_s / \lambda_{ab}^2(0)$ (Eq.(4)) require ξ_{c0} to fall off from its limiting value $\xi_{c0} = (R_2/f) d_s$. The doping dependence of ξ_{c0} in $\text{La}_{2-x}\text{Sr}_x\text{CuO}_4$, deduced from Eq.(13) and the experimental data for T_c and $\lambda_{ab}^2(0)$ is displayed in Fig.9a in terms of T_c *vs.* ξ_{c0} and ξ_{c0} *vs.* x . Approaching the underdoped limit ($x \approx 0.05$), where T_c vanishes (Fig.1) and the 2D-QSI transition occurs, ξ_{c0} increases nearly linearly with decreasing x to approach a fixed value. Indeed, the data is consistent with

$$\xi_{c0} = (16\pi^3 k_B / (\Phi_0^2 f)) T_c \lambda_{ab}^2(0) \approx 14.34 - 60.47(x - 0.05)\text{\AA}, \quad (14)$$

yielding the limiting value $\xi_{c0}(x = 0.05) \approx 14.34\text{\AA}$ and $f\xi_{c0}(x = 0.05) = R_2 d_s \approx 6.5\text{\AA}$ used in Fig. 8. An essential result is that ξ_{c0} adopts in the underdoped limit ($x \simeq 0.05$) where the 2D-QSI transition occurs and T_c vanishes its maximum value $\xi_{c0} \approx 14.34\text{\AA}$, which is close to the c-axis lattice constant $c \simeq 13.29\text{\AA}$. Thus, a finite transition temperature requires a reduction of ξ_{c0} , well described over an unexpectedly large doping range by Eq.(14). Noting that this relation transforms with Eq.(2) to

$$\xi_{c0} \approx 14.34 - 60.47\gamma_0/\gamma\text{\AA}, \quad (15)$$

this behavior is intimately connected to the doping dependence of the anisotropy. Hence, a finite T_c requires unavoidably a finite anisotropy γ . The lesson is, in agreement with the empirical relation (3), that superconductivity in $\text{La}_{2-x}\text{Sr}_x\text{CuO}_4$ is an anisotropic but 3D phenomenon which disappears in the 2D limit. From the plot $1/\lambda_{ab}^2(0)$ *vs.* T_c/ξ_{c0} displayed in Fig. 9b, where according to Eq.(13) universal behavior is expected to occur, the data is seen to fall rather well on a straight line. This is significant, as moderately underdoped, optimally and overdoped $\text{La}_{2-x}\text{Sr}_x\text{CuO}_4$ falling according to Fig. 8 well off the 2D-QSI behavior $T_c \propto 1/\lambda_{ab}^2(0)$ now scale nearly onto a single line. Thus the approximate 3D-XY scaling relation (13), together with the empirical doping dependence of the c-axis correlation length (Eqs.(14) and (15)) are consistent with the available experimental data for $\text{La}_{2-x}\text{Sr}_x\text{CuO}_4$ and uncovers the relevance of the anisotropy. However, the linear doping dependence of ξ_c is not expected to hold closer to the overdoped limit ($x \approx 0.27$) where T_c vanishes and a 3D quantum superconductor to normal state (3D-QSN) transition is expected to occur (see Fig.1).

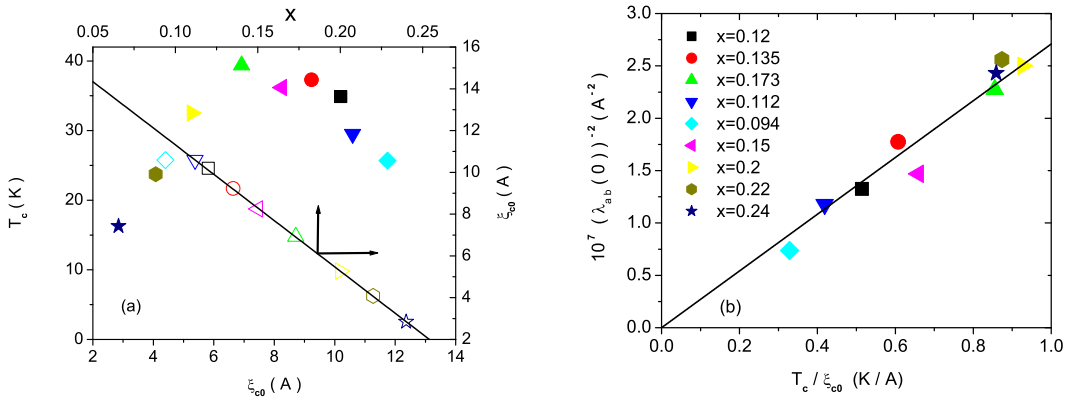


FIG. 9. (a) T_c *vs.* ξ_{c0} and ξ_{c0} *vs.* x for $\text{La}_{2-x}\text{Sr}_x\text{CuO}_4$. Data taken from Pangopoulos *et al.* [9] and Shibauchi *et al.* [8]. The solid line is Eq.(14). (b) $1/\lambda_{ab}^2(0)$ *vs.* T_c/ξ_{c0} for the same data with ξ_{c0} given by Eq.(14). The straight line is $1/\lambda_{ab}^2(0) = 2.71 T_c/\xi_{c0}$.

Since Eq.(11) is universal, it should hold for all cuprates falling in the accessible critical regime into the 3D-XY universality class, irrespective of the doping dependence of T_c , λ_{ab0}^2 , ξ_{ab0} , γ and ξ_{c0} . Having seen that charged criticality is accessible in the heavily underdoped regime only, Eq.(11) rewritten in the form

$$\frac{\xi_{c0}}{\lambda_{ab0}^2 T_c} = \frac{\xi_{ab0} \gamma}{\lambda_{c0}^2 T_c} = \frac{16\pi^3 k_B}{\Phi_0^2 f}, \quad (16)$$

provides a sound basis for universal plots. However, as aforementioned there is the serious drawback that reliable experimental estimates for the critical amplitudes and the anisotropy at T_c measured on the same sample and for a variety of cuprates are not yet available. Nevertheless, as in the case of $\text{La}_{2-x}\text{Sr}_x\text{CuO}_4$ outlined above, progress can be made by invoking the approximate scaling form (13) and by expressing the correlation lengths in terms of σ_i^{dc} the real part of the frequency dependent conductivity $\sigma_i^{dc}(\omega)$ in direction i extrapolated to zero frequency at $T \gtrsim T_c$ [69] in terms of

$$1/\xi_c \simeq \sigma_{ab}^{dc}/s_{ab}, \quad 1/(\gamma\xi_{ab}) \simeq \sigma_c^{dc}/s_c, \quad (17)$$

s_i with dimension Ω^{-1} incorporates the temperature dependence. With that the universal relation (16) transforms with Eq.(13) to

$$\frac{1}{\lambda_{ab}^2(0) T_c \sigma_{ab}^{dc}} \simeq \frac{1}{\lambda_c^2(0) T_c \sigma_c^{dc}} \simeq \frac{16\pi^3 k_B}{\Phi_0^2 f s_{ab}}, \quad (18)$$

because $\sigma_{ab}^{dc}/\sigma_c^{dc} = \gamma^2$ and with that $s_{ab} = s_c$. To check this relation we note that the 2D-QSI scaling from (4) transforms with the relation $d_s = \sigma^{sheet}/\sigma_{ab}^{dc}$ between sheet conductivity σ^{sheet} and conductivity σ_{ab}^{dc} to

$$\frac{1}{\lambda_{ab}^2(0) T_c \sigma_{ab}^{dc}} = \frac{16\pi^3 k_B}{\Phi_0^2 R_2 \sigma^{sheet}}, \quad \sigma^{sheet} = \frac{h}{4e^2} \sigma_0 \simeq \sigma_0 1.55 \cdot 10^{-4} \Omega^{-1}, \quad (19)$$

where $h/4e^2 = 6.45 \text{ k}\Omega$ is the quantum of resistance and σ_0 is a dimensionless constant of order unity [72]. Thus,

$$\frac{1}{\lambda_{ab}^2(0)} \simeq \frac{10.3 \cdot 10^{-5}}{R_2 \sigma_0} T_c \sigma_{ab}^{dc}, \quad (20)$$

with $\lambda_{ab}(0)$ in μm , T in K and σ_{ab}^{dc} in $(\Omega^{-1}\text{cm}^{-1})$, and the structure of the ab -expression in Eq.(18) is recovered. Similarly, approaching 2D-QSI criticality $\lambda_c(0)$ and σ_c^{dc} scale as [70]

$$\lambda_c(0) = \Omega_s (\sigma_c^{dc})^{-(2+z)/4}, \quad (21)$$

where $z = 1$ is the dynamic critical exponent of the 2D-QSI transition. Ω_s is a non-universal factor of proportionality. Noting that in this limit σ_c^{dc} and T_c scale as $T_c \propto (\sigma_c^{dc})^{z/2}$ the c -expression in Eq.(18) is readily recovered. Accordingly, there is no contradiction between the scaling forms (18) and (21). In this context it should be kept in mind that the universal relation is valid for the neutral case only. However we have seen that the effective dimensionless charge $\tilde{e}_{ab} = 1/\kappa_{ab}$ scales as $\tilde{e}_{ab} \propto T_c^{-1/2}$ and the charged critical regime becomes accessible. This is not the case for the c -axis penetration depth because $\tilde{e}_c \propto T_c^{3/2}$. For this reason, as the underdoped limit (2D-QSI transition) is approached there should be a crossover from Eq.(18) to the universal relation (19), becoming manifest in different constants on the right hand side.

On the other hand, approaching the 3D quantum superconductor to normal state (QSN) transition $\lambda_{ab,c}(0)$, T_c and $\sigma_{ab,c}^{dc}$ scale as [18] $1/\lambda_{ab,c}^2(0) \propto T_c^{(1+z)/z}$, $\sigma_{ab}^{dc} \propto T_c^{-(z_{cl}-1)/z}$, where z is the dynamic critical exponent of this quantum transition and z_{cl} the exponent associated with the finite temperature critical dynamics. Indeed, in this limit the correlation length ξ_τ associated with the finite temperature critical dynamics cannot be eliminated. Since ξ_τ scales as $\xi_\tau \propto \xi_{ab}^{z_{cl}}$ we obtain $\sigma_c^{dc} \propto \xi_c \xi_\tau / \xi_{ab}^2 \propto \xi_\tau / (\gamma \xi_{ab}) \propto \xi_{ab}^{z_{cl}-1} \propto T_c^{-(z_{cl}-1)/z}$. Accordingly,

$$\lambda_{ab}^2(0) T_c \sigma_{ab}^{dc} \propto \lambda_c^2(0) T_c \sigma_c^{dc} \propto T_c^{-z_{cl}/z} \quad (22)$$

should hold close to 3D-QSN criticality. Furthermore in this regime the effective charge becomes negligible small so that 3D-XY scaling applies. Indeed $\tilde{e}_{ab,c} = 1/\kappa_{ab,c}$ scales as $\tilde{e}_{ab,c} \propto T_c^{(z-1)/2z}$ because $\lambda_{ab,c} \propto T_c^{-(z+1)/2z}$ and $\xi_{ab,c} \propto T_c^{-1/z}$. A potential candidate for the 3D-QSN transition is the model proposed by Herbut [73]. It describes the disordered d-wave superconductor to disordered metal transition at weak coupling and is characterized by the dynamic critical exponents $z = 2$. When this holds true the effective charge scales at $\tilde{e}_{ab,c} \propto T_c^{-3/4}$ and 3D-XY scaling is no longer applicable. Furthermore there is experimental evidence for $z_{cl} = 2$ [51,74]. Accordingly, the scaling form (18) does not hold in the overdoped regime close to 3D-QSN criticality. In this regime Eq.(21) is replaced by [70]

$$\lambda_c(0) \propto (\sigma_c^{dc})^{\frac{1+z}{2(z_{cl}-1)}}, \quad (23)$$

with a non-universal factor of proportionality. What is particularly remarkable is then that the 3D-XY scaling from (18) predicts that all points of $1/\lambda_{ab}^2(0)$ vs. $T_c\sigma_{ab}^{dc}$ and $1/\lambda_c^2(0)$ vs. $T_c\sigma_c^{dc}$ should fall onto a single line with the exception of the overdoped regime where the scaling form (22) applies.

In Fig.10 we displayed $1/\lambda_{ab}^2(0)$ vs. $T_c\sigma_{ab}^{dc}$ and $1/\lambda_c^2(0)$ vs. $T_c\sigma_c^{dc}$ as collected by by Homes *et al.* [71]. In agreement with the scaling from (18) the *ab*-plane and *c*-axis data appears to be well described by the same line, namely $1/\lambda_{ab,c}^2(0) \simeq 5.2 \cdot 10^{-5} T_c\sigma_{ab,c}^{dc}$, yielding for $R_2\sigma_0$ in the 2D-QSI relation (Eq.(20)) the estimate $R_2\sigma_0 \cong 1.98$. Furthermore, all points of $1/\lambda_{ab}^2(0)$ vs. $T_c\sigma_{ab}^{dc}$ (open symbols) nearly fall onto a single line with a slope of unity. This is significant, as moderately underdoped, optimally and overdoped materials, which fell well off of the 2D-QSI behavior $T_c \propto 1/\lambda_{ab}^2(0)$ (see Eq.(4) and Fig.8) now scale nearly onto a single line, in agreement with Fig. 9b.

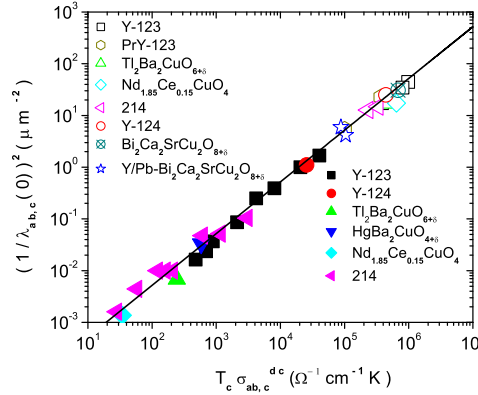


FIG. 10. $1/\lambda_{ab}^2(0)$ vs. $T_c\sigma_{ab}^{dc}$ (open symbols) and $1/\lambda_c^2(0)$ vs. $T_c\sigma_c^{dc}$ (full symbols) for various cuprates as collected by Homes *et al.* [71]. The straight line is $1/\lambda_{ab,c}^2(0) = 5.2 \cdot 10^{-5} T_c\sigma_{ab,c}^{dc}$. The experimental data is taken from [75–80] for $\text{YBa}_2\text{Cu}_3\text{O}_{7-\delta}$ (Y-123), [77] for $\text{Pr/Pb-YBa}_2\text{Cu}_3\text{O}_{7-\delta}$ (Pr/Pb-123), [78,81] for $\text{YBa}_2\text{Cu}_4\text{O}_8$ (Y-124), [78,81] for $\text{Tl}_2\text{Ba}_2\text{CuO}_{6+\delta}$, [77,82] for $\text{Bi}_2\text{Ca}_2\text{SrCu}_2\text{O}_{8+\delta}$ and $\text{Y/Pb Bi}_2\text{Ca}_2\text{SrCu}_2\text{O}_{8+\delta}$, [83,84] for $\text{Nd}_{1.85}\text{Ce}_{0.15}\text{CuO}_4$, [71,85] for $\text{La}_{2-x}\text{Sr}_x\text{CuO}_4$ (214), and [71] for $\text{HgBa}_2\text{CuO}_{4+\delta}$.

This agreement demonstrates that the approximate scaling relation 18 captures the essentials of the exact 3D-XY scaling form (16) by eliminating the doping dependence of the critical amplitudes towards the 2D-QSI transition in terms of their zero temperature counterparts. This evidence for anisotropic 3D-XY scaling raises again serious doubts that 2D models [36] are potential candidates to explain superconductivity in the cuprates. However the data does not extend sufficiently close to 2D-QSI- and 3D-QSN criticality in order to uncover the aforementioned crossovers from the scaling from (18) to (19) and from (18) to (22).

In contrast, the plot $\lambda_c(0)$ vs. σ_c^{dc} displayed in Fig. 11 provides according to the scaling form (21) information on the flow to 2D-QSI criticality. The straight line is Eq.(21) with $\Omega_s = 24$ appropriate for $\text{La}_{2-x}\text{Sr}_x\text{CuO}_4$ (214) and the arrow indicate the direction of this flow. The data for $\text{La}_{2-x}\text{Sr}_x\text{CuO}_4$ covers the range from $x = 0.08$ to 0.2 . Although the data is sparse one anticipates that the deviations from the straight line behavior increase systematically as the overdoped region is approached. As noted previously [70] this behavior is attributable to the initial crossover to 3D-QSN-criticality, where the scaling form (23) applies. Clearly more experimental data extending much closer to the overdoped limit are needed to uncover this crossover. Actually this also applies to the crossover from the scaling form (18) to (22).

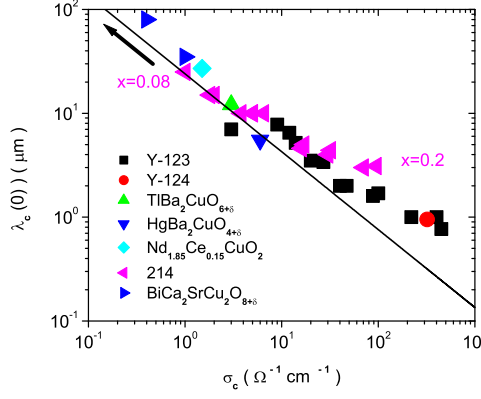


FIG. 11. $1/\lambda_c(0)$ vs. σ_c^{dc} using the data shown in Fig. 10 and taken from [86,87] for $\text{YBa}_2\text{Cu}_3\text{O}_{7-\delta}$ (Y-123), $\text{La}_{2-x}\text{Sr}_x\text{CuO}_4$ (214), and from [88] for $\text{Bi}_2\text{Ca}_2\text{SrCu}_2\text{O}_{8+\delta}$. The straight line corresponds to Eq.(21) with $\Omega_s = 24$ appropriate for $\text{La}_{2-x}\text{Sr}_x\text{CuO}_4$ (214).

Since Eq.(18), with the exception of the heavily overdoped regime, turned out to be nearly universal, it also implies that the changes ΔT_c , $\Delta(1/\lambda_{ab,c}^2)$ and $\Delta\sigma_{ab,c}^{dc}$, induced by pressure or isotope exchange are not independent, but related by

$$\frac{\Delta(1/\lambda_{ab,c}^2(0))}{(1/\lambda_{ab,c}^2(0))} = \frac{\Delta T_c}{T_c} + \frac{\Delta\sigma_{ab,c}^{dc}}{\sigma_{ab,c}^{dc}}. \quad (24)$$

In particular, for the oxygen isotope effect (^{16}O vs. ^{18}O) of a physical quantity X the relative isotope shift is defined as $\Delta X/X = (^{18}X - ^{16}X)/^{16}X$. Since close to 2D-QSI criticality $d_s = \sigma_{ab}^{sheet}/\sigma_{ab}^{dc}$ and with that $\Delta\sigma_{ab}^{dc}/\sigma_{ab}^{dc} = -\Delta d_s/d_s$ we recover the universal relation (5). Close to optimum doping where in $\text{YBa}_2\text{Cu}_3\text{O}_{7-\delta}$ $\Delta T_c/T_c = -0.26(5)\%$ and $\Delta(1/\lambda_{ab,c}^2(0))/(1/\lambda_{ab,c}^2(0)) = -5.6(2.0)\%$ [41] it predicts -5.6% effect on $\Delta\sigma_{ab}^{dc}/\sigma_{ab}^{dc}$ evaluated above and extrapolated to T_c . Hence, the absence of a substantial isotope effect on the transition temperature of cuprates does not rule out phonons as the bosons responsible for the coupling between the charge carriers, as previously suggested [89].

To summarize we observed remarkable agreement between the experimental data of underdoped cuprates and the flow to the 2D-QSI critical endpoint in the underdoped limit. Although an inhomogeneity induced finite size effect makes the asymptotic critical regime unattainable, there is considerable evidence that the 2D-QSI transition falls into the universality class of a 2D disordered bosonic system with long-range Coulomb interactions. The loss of superfluidity is due to the localization of the pairs, which ultimately drives the transition. Important implications include: (i) A finite transition temperature and superfluid density in the ground state are unalterably linked to a finite anisotropy. This finding raises serious doubts that 2D models [36] are potential candidates to explain superconductivity in cuprates. (ii) The doping dependence of the large oxygen isotope effects on the zero temperature in-plane penetration depth confirms the flow to 2D-QSI criticality, poses a fundamental challenge to this understanding and calls for a theory that goes beyond Migdal-Eliashberg. Although the majority opinion on the mechanism of superconductivity in the cuprates is that it occurs via a purely electronic mechanism involving spin excitations, and lattice degrees of freedom are supposed to be irrelevant, the relative isotope shift of the thickness of the superconducting sheets $\Delta d_s/d_s \approx 3.3(4)\%$ uncovers clearly the existence and relevance of the coupling between the superfluid and local lattice distortions. (iii) Given the striking feature that at low temperature the absolute change in $1/\lambda_{ab}^2$ and $1/\lambda_c^2$ has essentially no doping dependence, in contrast to $1/\lambda_{ab}^2(0)$ and $1/\lambda_c^2(0)$, scaling around the 2D-QSI critical endpoint implies a T^3 power law for $1/\lambda_c^2(T)$ and T for $1/\lambda_{ab}^2(T)$, consistent with experiment. Such power law behavior also follows from the nodes characteristic of a d-wave energy gap in the one particle density of states. However, our derivation shows that in underdoped cuprates these power laws are characteristic features of the 2D-QSI transition at the critical endpoint and hold for both s- and d-wave pairing. (iv) Similarly, we have seen that the large changes of $1/\lambda_{ab}^2(0)$, $1/\lambda_c^2(0)$ and T_c , consistent with the relation $T_c \propto \lambda_{ab}^{-2}(T=0) \propto \lambda_{ab}^{-2/3}(T=0)$, follow from the flow to the 2D-QSI criticality as well. (v) Because the Ginzburg parameters scale as $\kappa_{ab} \propto T_c^{1/2}$ and $\kappa_c \propto T_c^{-3/2}$ this flow was shown to open a door to observe charged criticality in the in-plane penetration depth at finite temperature. An

intriguing implications for microscopic models is then the increasing value of the effective charge of the pairs in the ab-plane, where $\tilde{e}_{ab} = 1/\kappa_{ab} \propto T_c^{-1/2}$, while in the c-direction it disappears as $\tilde{e}_c = 1/\kappa_c \propto T_c^{3/2}$. vi) We demonstrated here that the empirical relation $\lambda_{ab}^2(0) T_c \sigma_{ab}^{dc} = \lambda_c^2(0) T_c \sigma_c^{dc} \simeq \text{const}$ [71] is a consequence of 3D-XY universality extended to anisotropic systems. Nevertheless, these relations clearly reveal that the absence of a substantial isotope effect on the transition temperature of cuprates does not rule out phonons as the bosons responsible for coupling between the charge carriers, as previously suggested.

ACKNOWLEDGMENTS

The authors are grateful to D. Di Castro, R. Khasanov, S. Kohout, K.A. Müller, J. Roos and A. Shengelaya for very useful comments and suggestions on the subject matter. This work was partially supported by the Swiss National Science Foundation and the NCCR program *Materials with Novel Electronic Properties* (MaNEP) sponsored by the Swiss National Science Foundation.

-
- [1] M. Suzuki and M. Hikita, Phys. Rev. B **44**, 249 (1991).
 - [2] Y. Nakamura and S. Uchida, Phys. Rev. Phys. Rev. B **47**, 8369 (1993).
 - [3] Y. Fukuzumi, K. Mizuhashi, K. Takenaka, and S. Uchida, Phys. Rev. Lett. **76**, 684 (1996).
 - [4] M. Willemin, C. Rossel, J. Hofer, H. Keller, and A. Revcolevschi, Phys. Rev. B **59**, 717 (1999).
 - [5] T. Kimura, K. Kishio, T. Kobayashi, Y. Nakayama, N. Motohira, K. Kitazawa, and K. Yamafuji, Physica C **192**, 247 (1992).
 - [6] T. Sasagawa, Y. Togawa, J. Shimoyama, A. Kapitulnik, K. Kitazawa, and K. Kishio, Phys. Rev. B **61**, 1610 (2000).
 - [7] J. Hofer, T. Schneider, J. M. Singer, M. Willemin, H. Keller, T. Sasagawa, K. Kishio, K. Conder, and J. Karpinski, Phys. Rev. B **62**, 631 (2000).
 - [8] T. Shibauchi, H. Kitano, K. Uchinokura, A. Maeda, T. Kimura, and K. Kishio, Phys. Rev. Lett. **72**, 2263 (1994).
 - [9] C. Panagopoulos, J. R. Cooper, T. Xiang, Y. S. Wang and C. W. Chu, Phys. Rev. B **61**, 3808 (2000).
 - [10] J. L. Tallon, C. Bernhard, H. Shaked, R. L. Hitterman, and J. D. Jorgensen, Phys. Rev. B **51**, 12911 (1995).
 - [11] M. R. Presland, J. L. Tallon, R. G. Buckley, R. S. Liu, and N. E. Flower, Physica C **176**, 95 (1991).
 - [12] N. Momono, M. Ido, T. Nakano, M. Oda, Y. Okajima, and K. Yamaya, Physica C **233**, 395 (1994).
 - [13] T. Schneider, Acta Physica Polonica A **91**, 203 (1997).
 - [14] T. Schneider and J. M. Singer, *Phase Transition Approach To High Temperature Superconductivity*, Imperial College Press, London, 2000.
 - [15] T. Schneider and J. M. Singer, J. of Superconductivity **13**, 789 (2000).
 - [16] T. Schneider and H. Keller, Phys. Rev. Lett. **86**, 4899 (2001).
 - [17] T. Schneider, Physica B **326**, 289 (2003).
 - [18] T. Schneider, in *The Physics of Superconductors*, edited by K. Bennemann and J. B. Ketterson (Springer, Berlin 2004) p. xxx.
 - [19] L. Onsager, Phys. Rev. **65**, 117 (1944).
 - [20] J. Hofer, J. Karpinski, M. Willemin, G.I. Meijer, E.M. Kopnin, R. Molinski, H. Schwer, C. Rossel, and H. Keller, Physica C **297**, 103 (1998).
 - [21] G. Xiao, M. Z. Cieplak, J. Q. Xiao, and C. L. Chien, Phys. Rev. B **42**, 8752 (1990).
 - [22] J. M. Tarascon *et al.*, Phys. Rev. B **42**, 218 (1990).
 - [23] S. Watauchi, H. Ikuta, H. Kobayashi, J. Shimoyama, and K. Kishio, Phys. Rev. B **64**, 64520 (2001).
 - [24] T. R. Chien, W. R. Datars, B. W. Veal, A. P. Paulikas, P. Kostic, Chun Gu and Y. Jiang, Physica C **229**, 273 (1994).
 - [25] T. R. Chien, W. R. Datars, M. D. Lan, J. Z. Liu, and R. N. Shelton, Phys. Rev. B **49**, 1342 (1994).
 - [26] T. R. Chien and W. R. Datars, J. Z. Liu, M. D. Lan, and R. N. Shelton, Physica C **221**, 428 (1994).
 - [27] X. F. Sun, X. Zhao, X.-G. Li, and H. C. Ku, Phys. Rev. B **59**, 8978 (1999).
 - [28] C. Panagopoulos, J. R. Cooper, N. Athanassopoulou, and J. Chrosch, Phys. Rev. B **54**, 12721 (1996).
 - [29] P. A. Crowell, F. W. van Keuls, and J. R. Reppy, Phys. Rev. B **55**, 12620 (1997).
 - [30] Y. Uemura *et al.*, Phys. Rev. Lett. **62**, 2317 (1989).
 - [31] T. Schneider, Phys. Rev. B **67**, 134514 (2003).
 - [32] M. P. A. Fisher, G. Grinstein, and S. M. Girvin, Phys. Rev. Lett. **64**, 587 (1990).
 - [33] Min-Chul Cha, M. P. A. Fisher, M. Wallin, and A. P. Young, Phys. Rev. B **44**, 6883 (1991).
 - [34] I. F. Herbut, Phys. Rev. B **6**, 14723 (2000).

- [35] A. Hosseini, D.M. Broun, D.E. Sheehy, T.P. Davis, M. Franz, W.N. Hardy, Ruixing Liang and D.A. Bonn, cond-mat/0312542.
- [36] P. W. Anderson, P. A. Lee, M. Randeria, T. M. Rice, N. Trivedi, and F. C. Zhang, cond-mat/0311467.
- [37] J. Hofer, K. Conder, T. Sasagawa, Guo-meng Zhao, M. Willemin, H. Keller, and K. Kishio, Phys. Rev. Lett. **84**, 4192 (2000).
- [38] R. Khasanov, Studies of the oxygen-isotope effect on the magnetic field penetration depth in cuprate superconductors, Ph.D. Thesis, University of Zürich (2003).
- [39] R. Khasanov, A. Shengelaya, K. Conder, E. Morenzoni, I. M. Savic, and H. Keller, J. Phys.: Condens. Matter **15**, L17 (2003).
- [40] R. Khasanov, A. Shengelaya, E. Morenzoni, M. Angst, K. Conder, I. M. Savic, D. Lampakis, E. Liarokapis, A. Tatsi, and H. Keller, Phys. Rev. B **68**, 220506(R) (2003).
- [41] R. Khasanov, D. G. Eshchenko, H. Luetkens, E. Morenzoni, T. Prokscha, A. Suter, N. Garifanov, M. Mali, J. Roos, K. Conder, and H. Keller, Phys. Rev. Lett. **92**, 057602-1 (2004).
- [42] A. B. Migdal, Sov. Phys. JETP **7**, 996 (1958); G. M. Eliashberg, Sov. Phys. JETP **11**, 696 (1960).
- [43] T. Schneider, cond-mat/0308595.
- [44] K. Conder *et al.*, in *Phase Separation in Cuprate Superconductors*, edited by E. Sigmund and K. A. Müller (Springer, Berlin 1994) p. 210.
- [45] F. Raffa, T. Ohno, M. Mali, J. Roos, D. Brinkmann, K. Conder, and M. Eremin, Phys. Rev. Lett. **81**, 5912 (1998).
- [46] E.I. Maksimov, Zh. Eksp. Teor. Fiz. **37**, 1562 (1969).
- [47] J. P. Carbotte, Rev. Mod. Phys. **62**, 1027 (1990).
- [48] A. Paramekanti, M. Randeria, and N. Trivedi, cond-mat/0305611.
- [49] D. S. Fisher, M. P. A. Fisher and D. A. Huse, Phys. Rev. B **43**, 130 (1991).
- [50] T. Schneider and D. Ariosa, Z. Phys. B **89**, 267 (1992).
- [51] T. Schneider and H. Keller, Int. J. Mod. Phys. B **8**, 487 (1993).
- [52] S. Coleman and E. Weinberg, Phys. Rev. D **7**, 1988 (1973).
- [53] B. I. Halperin, T. C. Lubensky, and S. K. Ma, Phys. Rev. Lett. **32**, 292 (1974).
- [54] C. Dasgupta and B. I. Halperin, Phys. Rev. Lett. **47**, 1556 (1981).
- [55] S. Kolnberger and R. Folk, Phys. Rev. B **41**, 4083 (1990).
- [56] M. Kiometzis, H. Kleinert, and A. M. J. Schakel, Phys. Rev. Lett. **73**, 1975 (1994); Fortschr. Phys. **43**, 697 (1995).
- [57] I. F. Herbut and Z. Tesanovic, Phys. Rev. Lett. **76**, 4588 (1996).
- [58] I. F. Herbut, J. Phys. A **30**, 423 (1997).
- [59] P. Olsson and S. Teitel, Phys. Rev. Lett., **80**, 1964 (1998).
- [60] J. Hove and A. Sudbø, Phys. Rev. Lett., **84**, 3426 (2000).
- [61] S. Mo, J. Hove, A. Sudbø, Phys. Rev. B **65**, 104501 (2002).
- [62] S. Kamal, D. A. Bonn, N. Goldenfeld, P. J. Hirschfeld, R. Liang, and W. N. Hardy, Phys. Rev. Lett. **73**, 1845 (1994); S. Kamal, R. Liang, A. Hosseini, D. A. Bonn, and W. N. Hardy, Phys. Rev. B **58**, R8933 (1998).
- [63] T. Schneider, R. Khasanov, K. Conder, and H. Keller, J. Phys. Condens. Matter **15**, L763 (2003).
- [64] T. Schneider, Journal of Superconductivity, **17**, 41 (2004).
- [65] T. Schneider and D. Di Castro, Phys. Rev. B **69**, 024502 (2004).
- [66] T. Schneider, R. Khasanov, K. Conder, E. Pomjakushina, and H. Keller, to be published.
- [67] Y.J. Uemura *et al.*, Phys. Rev. B **38**, 909 (1988).
- [68] A. Peliasetto and E. Vicari, Physics Reports **368**, 549 (2002).
- [69] C. C. Homes, S. V. Dordevic, D. A. Bonn, Ruixing Liang, W. N. Hardy, and T. Timusk, cond-mat/0312211.
- [70] T. Schneider, Europhys. Lett., **60**, 141 (2002).
- [71] C. C. Homes, S. V. Dordevic, M. Strongin, D. A. Bonn, Ruixing Liang, W. N. Hardy, Seiki Koymia, Yoichi Ando, G. Yu, X. Zhao, M. Greven, D. N. Basov, and T. Timusk, cond-mat/0404216.
- [72] I. F. Herbut, Phys. Rev. Lett. **81**, 3916 (1998).
- [73] I. F. Herbut, Phys. Rev. Lett. **85**, 1532 (2000).
- [74] K. D. Osborn, D. J. Van Harlingen, Vivek Aji, Nigel Goldenfeld, S. Oh, and J. N. Ecks, Phys. Rev. B **68**, 144516 (2003).
- [75] D. N. Basov *et al.*, Phys. Rev. Lett. **74**, 598 (1995).
- [76] C. C. Homes *et al.*, Phys. Rev. B **60**, 9782 (1999).
- [77] H. L. Liu *et al.*, J. Phys: Condens. Matter **11**, 239 (1999).
- [78] D.N. Basov, T. Timusk, B. Dabrowski, and J. D. Jorgensen, Phys. Rev. B **50**, 3511 (1994).
- [79] C. C. Homes, T. Timusk, D. A. Bonn, R. Liang, and W. N. Hardy, Physica C **254**, 265 (1995).
- [80] J. Schützmann, S. Tajima, S. Miyamoto, and S. Tanaka, Phys. Rev. Lett. **73**, 174 (1994).
- [81] A. V. Puchkov, T. Timusk, S. Doyle, and A. M. Herman, Phys. Rev. B **51**, 3312 (1995).
- [82] D. N. Basov, *et al.*, Science **283**, 4952 (1999).
- [83] C. C. Homes, B. P. Clayman, J. L. Peng, and R. L. Greene, Phys. Rev. B **56**, 5525 (1997).
- [84] E. J. Singley, D. N. Basov, K. Kurahashi, T. Uefuji, and K. Yamada, Phys. Rev. B **64**, 224 (2001).
- [85] T. Startseva *et al.*, Phys. Rev. B **59**, 7184 (1999).
- [86] S. Uchida and K. Tamasaku, Physica C **293**, 1 (1997).

- [87] T. Motohashi, J. Shimoyama, K. Kitazawa, K. Kishio, K. M. Kojima, and S. Uchida, Phys. Rev. B **61**, 9269 (2000).
- [88] H. Shibata and A. Matsuda, Phys. Rev. B **59**, 11672 (1999).
- [89] J. P. Franck, in *Physical Properties of High Temperature Superconductors III*, edited by D. M. Ginsberg (World Scientific, Singapore, 1994).